sea surface temperature (SST) and chlorophyll-a data. Primary data consisted of hydroacoustic and CTD data sourced from field data acquisition of the BUDEE 2022 study. Meanwhile, secondary data consists of Himawari-8 image data from the Japan Meteorological Agency (JMA) downloaded through JAXA.

2.3 Hydroacoustic data processing

Calculation of fish density requires a value of Target Strength (TS) and Volume backscattering strength (Sv). TS as a result of single organism detection while Sv from group organism or fish density [7]. SV and TS values are logarithmic values (dB) obtained from the recorded data. To calculate the density of fish, through the process of Echo-Integration in the ESP3 application can be generated variable $\overline{TS}, \overline{Sv}, \& Sa$ and then processed in Microsoft Excel. The Sv value can be found using the equation [8] :

$$\rho A = \left(\frac{Sa}{\overline{\sigma_{bs}}}\right) \times 10^6 \quad (1)$$

where,
ρA : Fish Density (fish/km^{-2})
Sa : *Backscattering Coefficient Area* (m^{2}m^{-2})
σ_{bs} : *Backscattering Cross-section* Average (m^2)

Sa is obtained from equation 2 [9] :

$$Sa = 10^{\left(\frac{\overline{SV}}{10}\right)} \times \bar{T} \quad (2)$$

where,
Sa : *Backscattering Coefficient Area* (m^2 m^{-2})
$\overline{Sv}$: Average Volume *Backscattering Strength* (m2 m-3)
$\bar{T}$: Average water column thickness

The $\overline{\sigma_{bs}}$ and $\overline{Sv}$ are the average of Sv and σ_{bs} obtained from equations 3 and 4..

$$Sv = 10^{\left(\frac{(SV)}{10}\right)} \quad (3)$$

$$\sigma_{bs} = 10^{\left(\frac{(TS)}{10}\right)} \quad (4)$$

dimana,
Sv : *Backscattering Coefficient* Volume (m^2 m^{-3})
SV : *Backscattering Strength* Volume (dB re 1 m^2) abundance
σ_{bs} : *Backscattering Cross Section* Average (m^2)
TS : *Target Strength* Average (dB re 1 m^2)

One factor that greatly influences the TS value is fish size. Fish length (L) is linearly related to the scattering cross section (σbs = aLb). To convert the fish target strength value into fish length (L), the following equation is used [10]:

$$TS = 20 \log L - 68 \, (db) \quad (5)$$

where,
TS : Average Target Strength (dB re 1 m^2)
L : Fish length (cm)

2.4 Satellite image data processing

In this study, Himawari level 3 satellite image data in NetCDF (ncFile) format with a spatial resolution of 2 km for Sea Surface Temperature (SST) data and 5 km for chlorophyll data, with temporal resolution every hour. Himawari level 3 satellite image data has been spatially corrected, so that no manual correction is made by the user. Furthermore, IDW interpolation is performed to complete the "NoData" area in the Himawari-8 data. The IDW method shows good performance in predicting missing image data [11]. Chlorophyll-a and Sea Surface Temperature data from Himawari-8 images are first processed using SeaDAS to extract chlorophyll-a values from Himawari-8 images. The processed data from SeaDAS is stored in TIFF form so that it can be processed in ArcGIS. The results of the fishing potential zone are obtained from the overlay of chlorophyll-a and sea surface temperature data of Himawari-8 Level 3 images that are reclassified into predetermined classes [12]. The results of the analysis of sea surface temperature and chlorophyll-a will then be calculated relative error value against field data, namely CTD data. The calculation is done as a validation test to determine whether sea surface temperature and chlorophyll-a data can be used in determining potential fishing zones. The relative error value is obtained from the following formula [13]:

$$RE = \left[\frac{Xinsitu - Xcitra \; x \; 100\%}{N} \right]$$

Description:
RE : Relative Error
X*insitu* : field measurement data
X*citra* : data from satellite imagery
N : amount of data

ZPPI points were then identified through spatial analysis using the overlay method. The overlay method incorporates contours from the IDW results of SPL and chlorophyll-a data. Then, an analysis was carried out to see the correlation between sea surface temperature and chlorophyll-a values at the identified fish density points, using Generalized Additive Model (GAM) modeling as follows [14]:

$$g(\mu i) = Ai\theta + s(TEMP) + s(SSC) + s(SA + s(SSH) \quad (6)$$

Description:
g = *link function*
μi = predicted value of the dependent variable
$Ai\theta$ = koefisien konstanta
s = *smooting function*

3 Results and discussion

3.1 Fish density distribution of hydroacoustic calculation results

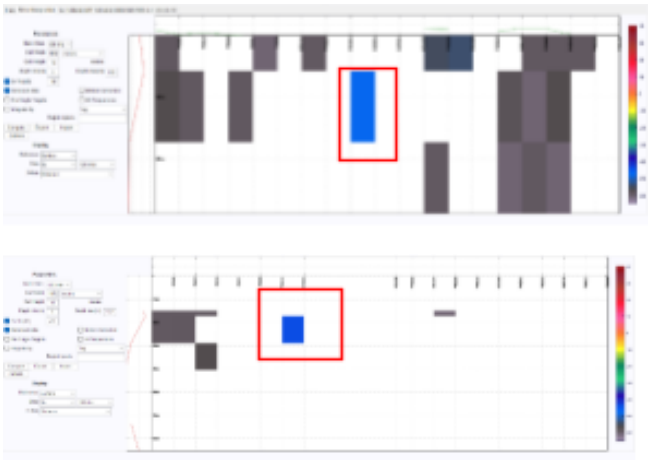

Fig. 2. Echo Integration Identified as Having SV Value on ESP3 Echogram.

Figure 2 shows the echogram from the hydroacoustic data processing at ESP3. Data processing is done by maximizing the analysis to 200 m below the sea surface. Based on the results of processing in ESP3, an echo integration bin is obtained which has an Sv value that indicates the presence of fish density. On the echogram, the echo integration bin that has an Sv value is identified as a blue area/mark. The distribution of fish density is then mapped spatially and displayed with visualization using a heatmap in the figure 6. In the heatmap map of fish density distribution, 3 dense points were identified. The highest valid echo integration bin frequency is found in the path section for data dated September 10, 2022 at 10:00 to 16:00 in the northeast of Banggai Island, Banggai Islands Regency. Then at the end of the path (c), the valid echo integration bin density appears to be lower until the end of the path. The end of this path is the track of the data dated September 11 at 01:00 in the upper part of the entire track.

The spatial distribution of fish density tends to be in the Banggai Waters area close to the coast of the Banggai Peninsula, Banggai Regency, Central Sulawesi. The class of fish density that appears dominantly in is [500 - 1,000 fish/km^2], namely as many as 6 points. Overall, it has a very high fish density with a total estimated density of 23,39.79 fish/km^2. Meanwhile, the highest density overall was 7,745.955 fish/km^2 and this was the column in the recording data on 10 September at 16:00. The mean TS values detected ranged from -53.57 dB re 1 m^2 to -36.36 dB re 1 m^2.

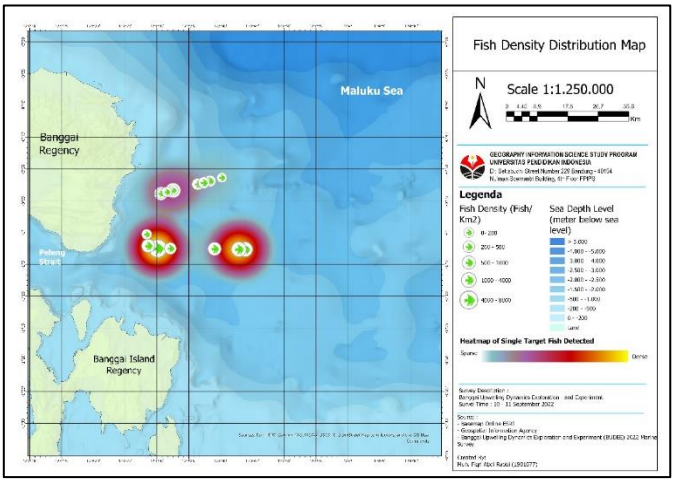

Fig. 3. Fish Density Distribution Map.

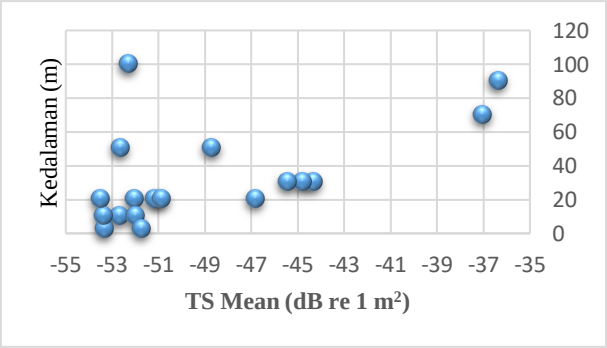

Fig. 4. Scatter Plot of the relationship between TS Mean values for echo integration and depth.

Figure 4 shows a scatter plot of the relationship between Mean TS values with depth and fish length. The conversion of TS values to fish length follows the classification [10,18]. The mean TS values detected in the range of -55 dB re 1 m2 to -43 dB re 1 m2 tended to be at depths of 0 m to -40m. The other mean TS values in the range of -53 dB re 1 m^2 to -47 dB re 1 m^2 and -39 dB re 1 m^2 to -35 dB re 1 m^2 are detected at depths of -60 m to -100 m, respectively. Meanwhile, the mean TS values are concentrated in the range of -55 dB re 1 m^2 to -51 dB re 1 m^2 at depths of 0-20 m. The highest values of estimated density by size were in the very small (<6 cm) and small (6 cm to 20.89 cm) fish categories, which were estimated at 19,048 fish km^2 and 2,053 fish km^2, respectively. As for the medium fish category (20.89 - 58.88 cm), it has the second highest density value with a fish density value of 2,297 km^2. The overall total fish density value obtained was 23.398 km^2. The estimation results of fish density estimation based on TS value and fish size can be seen in Table 1 below.

Table 1. Estimation of fish density based on TS value and fish size.

TS Value Mean (dB re 1 m^2)	Fish Length (cm)	Fish Category	Fish Density (Fish/km^2)
<50	< 6	Very Small	19,048
50 – 47	6 - 10.47	Small	1,310

47 – 44	10.47 - 14.79	Small	128
44 – 41	14.79 - 20.89	Small	615
41 – 38	20.89 – 29.52	Medium	204

3.2 Distribution of chlorophyll-a and sea surface temperature

Based on the mapping results, the distribution of chlorophyll-a is concentrated in the western part of the Maluku Sea, which includes the Banggai Waters and the Peleng Strait as shown in Figure 5. However, the distribution also fluctuates from time to time. From the overall data, it can be seen that the highest chlorophyll-a value is 2.94 mg/m³ at 10:00 on September 10, 2022 and the lowest is on September 11, 2022 at 01:00 which is 0.01 mg/m³. From the three maps, the distribution of chlorophyll-a at all three times has a value that has the potential as a ZPPI, which is at 0.2 - 2mg/m³ [15]. The closest range is processed chlorophyll using satellite imagery with the lowest value being 0.29 mg/m³ and the highest being 2.94 mg/m³. The range of Chlorophyll-a that has the potential for fishing potential zones and is very high is at 0.2-2mg/m³[15].

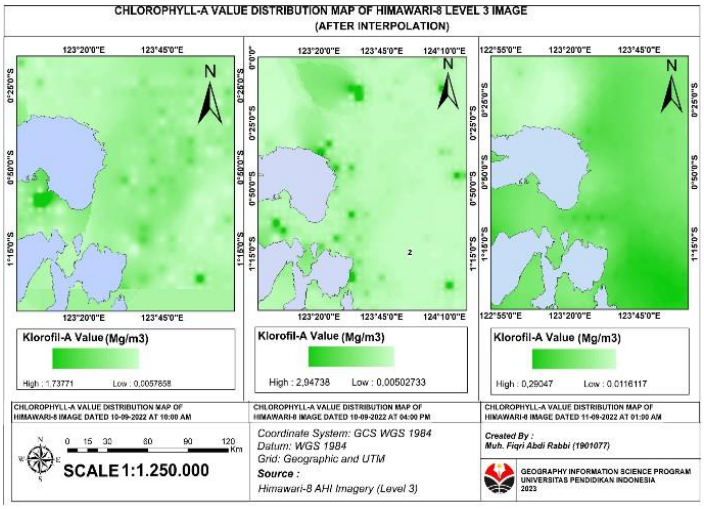

Fig. 5. Map of Chlorophyll-A Value Distribution of Himawari-8 Image.

Meanwhile, the distribution of sea surface temperature as shown in Figure 3 tends to be constant, namely low sea surface temperatures concentrated in the southern part of Banggai Waters and around the Banggai Islands Regency to Tolo Bay. The highest sea surface temperature value occurred at 16:00 on September 10, 2022, namely 29.54 ° C and the lowest value was 24.71 ° C at 01:00 on September 11, 2022. Based on sea surface temperature values at the three time in this study, there is great potential for the presence of fish because the value of sea surface temperature obtained is in the optimal category (25.31°C). sea surface temperature obtained is in the optimal category (25.31°C) [15]. Potential fish locations based on sea surface temperature data data are scattered in the waters around the Banggai Islands Regency, the waters around the Banggai Laut around Banggai Laut Regency, Peleng Strait and Tolo Bay. As a form of accuracy test of the image data used, a choreography analysis of the

measurement of oceanographic parameters from the image results with in situ data derived from CTD data was carried out.

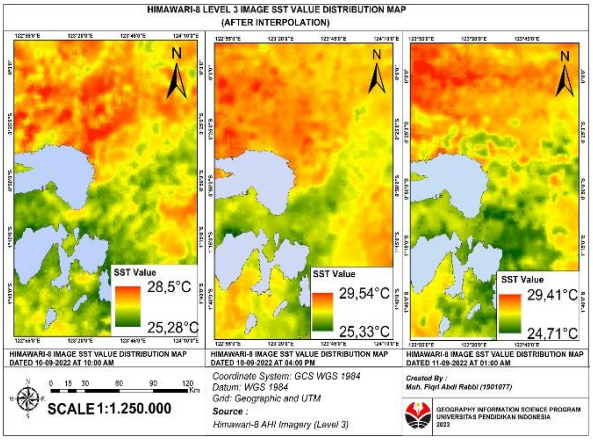

Fig. 6. Map of Sea Surface Temperature Value Distribution of Himawari-8 Image.

Measurement of Sea Surface Temperature (SPL) and Chlorophylla from CTD in situ data coincides with the time of hydroacoustic data acquisition, namely on September 10-11, 2022. Based on the calculation results, the relative error value between the measurement of sea surface temperature data from images and in situ data has an average relative error value of 0.11%, while Chlorophyll-a data has a relative error value of 13.46%. Based on previous research, less than 30% of image data processing can be used for further analysis, many factors cause errors, one of which is the quality of the image data used and errors during observation and in situ data acquisition [13,16-17]. The verification results are shown in table 2 here

Table 2. Estimation of fish density based on TS value and fish size.

Time Observation	CTD Data		Imagery Data		Value Error (%)	
	SPL	CHL	SPL	CHL	SPL	CHL
05:00 AM - 10:00 AM Sep 10, 2022	26.61	0.44	27.31	0.14	2.63	19.08
11:00 AM - 8:00 PM Sep 10, 2022	27.86	0.18	27.74	0.21	0.44	11.28
9:00 PM Sep 10, 2022 - 3:00 AM Sep 11, 2022	27.73	0.24	27.21	0.14	1.85	10.02
Mean Relatives Error					13.46	0.11

3.3 Mapping fishing potential zones

Based on the results of the processed zoning map of fishing potential (ZPPI), it is concluded that the area in Banggai Waters has a high potential for the presence of fish, the concentration of high category ZPPI in the waters to the southwest and northeast of Banggai.

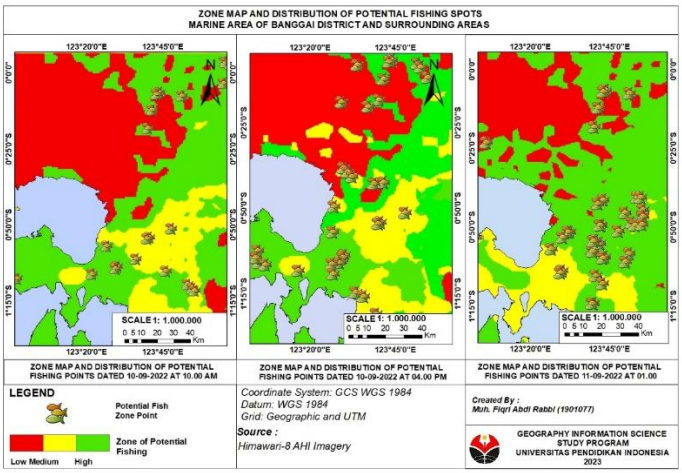

Fig. 7. Map of Fishing Potential Zones.

On the fishing potential zone map as shown in Figure 7, the central part of Banggai Waters has a medium category ZPPI and there is a high category in the waters of Peleng Strait to Tolo Bay at 10:00 and 16:00 on September 10, 2022. However, this changed at 01.00 on September 11, 2022, namely the Central Banggai Waters area entered the high category and the medium category shifted to the waters of Peleng Strait and Tolo Bay. Meanwhile, the low ZPPI level is consistently distributed in Tomini Bay and southeastern Banggai Waters. Even so, there is a small portion of Tomini Bay waters that fall into the medium ZPPI category at 16:00 on September 10, 2022 near the coast of the Banggai Peninsula.

Overall, from the results of mapping the potential fishing zones, the high category has the highest percentage of 43%, the second category is low at 28% and finally the medium category at 29%. These results are based on variables and classification of ZPPI potential [12,15]. The low category has a variable high sea surface temperature of 30-32°C and low chlorophyll-a 00.1 mg/m³, the medium category has a medium sea surface temperature of 29-30°C and medium chlorophyll-a 0.11-1 mg/m³, the high category has a low sea surface temperature of 24-28°C and high chlorophyll-a 1-12 mg/m³.

Then for the distribution of ZPPI points concentrated in the Southern Banggai Waters. The most ZPPI points at 16:00 on September 10, 2022. ZPPI points are widely spread on the coast of the Banggai Peninsula, Banggai Islands, to the Peleng Strait. These ZPPI points are scattered mostly in the high category ZPPI, the rest, a small portion, are in the medium category ZPPI. Meanwhile, at 10:00 a.m. on September 10, 2022 the ZPPI points are scattered on the coast of the Banggai Peninsula to the central Banggai Waters and the northern part of the Maluku Sea. ZPPI points at 10:00 on September 10, 2022 are evenly distributed in all ZPPI categories. Furthermore, at 01:00 on September 11, 2022, it was spread very dominantly in the central part of Banggai Waters. This ZPPI point research time is spread most dominantly in the high ZPPI category compared to other research times.

In analyzing the validation of potential fishing zones using a comparison of the results of mapping the distribution of fish density data from the results of hydroacoustic calculations, it can be seen that the results of ZPPI mapping are quite consistent with the results of fish density data. This can be identified from 19 fish density points that overlap and/or are adjacent to the ZPPI point, of which 13 points are in the high category ZPPI.

Of all the fish density points detected, the majority are in the range of 200 - 1000 km2, namely 11 densities and are in the high ZPPI category. The correlation of the distribution of fish density points and ZPPI points on the basis of proximity to the location and correlation with the zoning of potential fishing areas that show most of the fish density points are in the high category, indicating that the results of the mapping of potential fishing zones are accurate enough to be used as a reference in determining potential points and zones to be used as fishing areas.

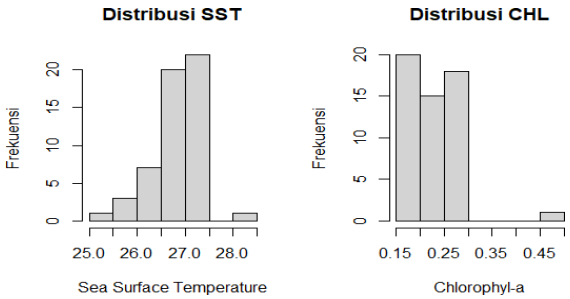

Fig. 8 Histogram of Frequency Distribution of Sea Surface Temperature and Chlorophyll-a Values at Identified Fish Density Points.

Then, the analysis of the relationship between sea surface temperature and Chlorophyll-a with the identified fish density points was carried out using the Generalized Additive Model (GAM) modelling. The distribution of sea surface temperature and Chlorophyll-a values at fish density points can be seen in Figure 8. The relationship between fish density results and oceanographic parameters can be determined using the Generalized Additive Model (GAM) statistical modelling analysis. The relationship between fish density values and oceanographic parameters of identified fish density points is presented in the form of a histogram (Figure 7). The histogram was formed to determine the value of oceanographic parameters in the fishing grounds of the identified fish density points. Sea surface temperature values at fish density points are in the range of 2528°C with the highest accumulated value being in the range of 27°C. Meanwhile, the Chlorophyll-a concentration has the highest value of 0.1 - 0.3 mg/m3 and is in the range of 0.15 - 0.45 mg/m^3.

The GAM model is formed with one response variable followed by a combination of two predictor variables. From these two variables, 3 prediction models were formed which are shown in table 3. Of all the models developed, the model with the highest potential was determined by looking at the results of Akaike's Information Criterion (AIC) and Cumulative Deviance Explained (CDE). The model with the lowest AIC value and the highest CDE has the highest level of accuracy in explaining the response variable. A comparison of the AIC and CDE values of the three models can be seen in Table 3.

Table 3. Common criteria fishing vessel stability.

Mode l	Variabel	pValue	Fish Density (Fish/km^2)	CDE (%)
SST	SST	0.683**	389.5436	0.87
CHL	CHL	0.36**	389.0608	16.2
SST + CHL	SST + CHL	0.509** 0.328**	387.652	18.4

The model with a combination of two parameters (Chlorophyll-a and sea surface temperature) has the smallest AIC value of 387.652 with the largest CDE of 18.4%. This shows that the model is the most potential model to determine the optimal fish catch area. The value of The CDE obtained from this model is 18,4%. The parameter that has a positive effect on density is seen from the significance

value of 0.328. The significance value of Chlorophyll-a obtained is close to zero. Meanwhile, the parameter with the sea surface temperature model as a single variable is a parameter that has the potential for low fish density. The significance value obtained from the sea surface temperature parameter is 0.683.

Chlorophyll-a parameter is a parameter that has a significant relationship with catch with a significance value of 0.328. Food available in the waters can be estimated by Chlorophyll-a content. A high concentration of Chlorophyll-a in a body of water will increase plankton productivity, thus creating a food chain in the water [19]. Chlorophyll-a values require time or time lag for large fish species [20]. Therefore, based on the GAM results, it is concluded that Chlorophyll-a is one of the main factors affecting the variability and distribution of fish density in the study area.

The results of the GAM statistics, shown on the smoothing curve, show that the range of values of the oceanographic paramater variables can have a positive influence on the response variable. The solid black line shows the corresponding GAM function, which describes the effect of the predictor variable on the response variable (fish density). If the GAM function obtained is above the zero value, then the percentage value is positive, indicating a strong influence of the parameter. Conversely, if the GAM function is below the zero axis, it indicates that the effect of the parameter on fish density is negative or weak.

The rug plot on the x-axis shows the relative density of the data points. GAM modeling calculations were obtained using the "gam" function in R software. From the GAM plots formed, sea surface temperature has a positive influence on the distribution of fish represented by the "effects pa" axis in the range of 26.5 to 27°C and the Chlorophyll-a concentration interval is in the range of 0.18 to 0.27 mg/m3. These modeling results are in accordance with the criteria [15], which shows that the optimal oceanographic parameter criteria for potential fishing areas are at temperatures of 24-28 °C and chlorophyll-a concentration values of 0.2 - 2 mg/m3. From the GAM smoothing curve graph, it can also be seen that the value of the high confidence level in the range of temperature and Chlorophyll-a concentration is positively correlated. This can be seen from the gray shaded area that is very minimal in the value range.

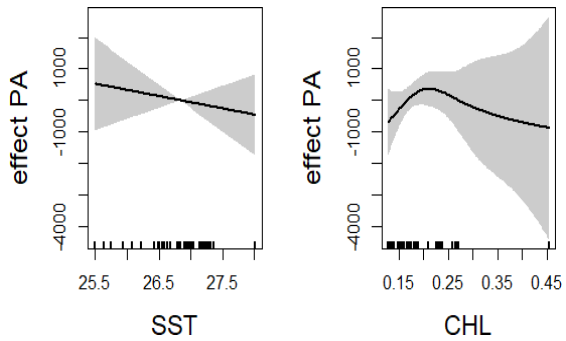

Fig. 9. Histogram of Frequency Distribution of Sea Surface Temperature and Chlorophyll-a Values at Identified Fish Density Points.

4 Conclusion

The results of the mapping of fishing potential zones show that the high category has the highest percentage (43%), followed by the low (28%) and medium (29%) categories. The point distribution map of the potential fishing zones shows a concentration of ZPPI points in the southern Banggai waters, especially close to the coast of the Banggai Peninsula. Fish density distribution tends to congregate in the area. The correlation between the distribution of fish density points, ZPPI points, sea surface temperature, and chlorophyll-a shows fairly accurate modelling results. This confirms that ZPPI mapping can be used as a guide to determine potential points or zones in fishing.

References

1. Y. Adel, M.F. Rahardjo, Indonesian Journal of Agricultural Sciences, **21**(3), 186-194. (2016)
2. Central Bureau of Statistics of Banggai Regency, *Banggai District in Figures 2022* (Central Bureau of Statistics of Banggai Regency, Banggai Regency, 2022)
3. H.M. Manik, in Proceedings of the Indonesian National Fisheries Seminar, 19-24 Jakarta, Indonesia (2013)
4. H. Priyadi, Spatial approach to determine potential areas of large pelagic fish presence in Banggai waters, Central Sulawesi Province (University of Indonesia, Jakarta, 2015).
5. A. Ma'mun, A. Priatna, H. Herlisman, , Indonesian Journal of Fisheries Research, **24**(3), 197-208. (2018).
6. Ministry of Marine Affairs and Fisheries of the Republic of Indonesia, Marine and Fisheries in Figures 2020 (Ministry of Marine Affairs and Fisheries of the Republic of Indonesia, Jakarta, 2020).
7. M.Z. Lubis, H.M. Manik, , Journal of Geoscience, Engineering, Environment, and Technology,. **3**(2): 1-6 (2017)
8. J. Simmonds, D. MacLennan, *Fisheries Acoustics: Theory and Practice (2nd ed.)* (Blackwell Science., 2005)
9. Y. Ladroit, P.C. Escobar-Flores, Schimel, A. C., & O'Driscoll, R. L., SoftwareX, **12**, 100581 (2020)
10. K.G. Foote, J. Acoust. Soc. Am. **82**(3): 981-987. (1987)
11. Kusuma, D. W., Murdimanto, A., Sukresno, B., & Jatisworo, JFMR (Journal of Fisheries and Marine Research), **2**(2), 103-115. (2018).
12. S. Karuppasamy, T.P. Ashitha, R. Padmanaban, M. Shamsudeen, J.M.N. Silva, Indian Journal of Geo Marine Sciences. **49**(06), 1025-1030. (2020).
13. L.M. Jaelani, F. Setiawan, B. Matsushita, *Proceedings of the Annual Scientific Meeting*. **20**. 464-470. (2015)
14. S.N. Wood, *Generalized Addtive Models: An Introduction with R. Second* (CRC Press, 2017)
15. R. Clinton, I.W.G.A. Karang, Widiastuti, Indian Journal of Geo Marine Sciences. **49**(06), 1025-1030. (2022).
16. R.A.P. Sari, B.B. Jayanto, H.A. Setyawan, Journal of Fisheries Resources Utilization Management and Technology, **8**(3), 28-43 (2019)
17. BL. Simanjuntak, G. Handoyo, D. Nugroho, Journal Of Oceanography, **2**(1): 1-7. (2013)
18. D. Panggabean, R. Nazzla, Indonesian Journal of Fisheries Research, **28**(2), 61–75 (2022)
19. G. Ramdhan, D. Ernaningsih, M. Limbong, Satya Minabahari Scientific Journal, **8**(2), 29-42 (2023)
20. A.R. Puspita, M.L. Syamsuddin, Subiyanto, F. Syamsudin, N.P. Purba, Journal of Marine Science and Engineering, **11**(1), 165 (2023)